



Published in final edited form as:

*Circulation*. 2018 October 23; 138(17): 1828–1838. doi:10.1161/CIRCULATIONAHA.117.030718.

## Increased RTN3 leads to obesity and hypertriglyceridemia by interacting with HSPA5

Rong Xiang, PH.D<sup>1,#,\*</sup>, Liang-liang Fan, PH.D<sup>1,#</sup>, Hao Huang, PH.D<sup>1,#</sup>, Ya-qin Chen, M.D.<sup>2,#</sup>, Wanxia He, PH.D<sup>3</sup>, Shuai Guo, M.S<sup>1</sup>, Jing-Jing Li, M.S<sup>1</sup>, Jie-yuan Jin, M.S<sup>1</sup>, Ran Du, PH.D<sup>1</sup>, Riqiang Yan, PH.D<sup>3</sup>, and Kun Xia, PH.D<sup>1,\*</sup>

<sup>1</sup>Department of cell biology, School of Life Sciences, Central South University, Changsha 410013, China

<sup>2</sup>Department of Cardiology, the Second Xiangya Hospital of Central South University, Changsha, 410011, China

<sup>3</sup>Department of Neurosciences, Lerner Research Institute, Cleveland Clinic Foundation, Cleveland, OH 44195, USA

### Abstract

**Background**—Reticulon 3 (RTN3) is an endoplasmic reticulum protein that has been previously shown to play a role in neurodegenerative diseases, but little is known about its role in lipid metabolism.

**Methods**—Obesity patients (149), hypertriglyceridemia patients (343), and healthy controls (84) were enrolled to assess their levels of RTN3. To explore pathophysiological roles of RTN3 in the control of lipid metabolism, we utilized Tg-RTN3 and RTN3-null transgenic mouse models and multiple *C. elegans* strains for molecular characterization. The underlying mechanisms were studied using 3T3L1 cell cultures *in vitro*.

**Results**—We report that overexpressed RTN3 in mice induces obesity and higher accumulation of triglycerides (TGs). Remarkably, increased RTN3 expression is also found in patients with obesity and hypertriglyceridemia. We reveal that RTN3 plays critical roles in regulating the biosynthesis and storage of TGs and in controlling lipid droplet expansion. Mechanistically, RTN3 regulates these events through its interactions with HSPA5, and this enhanced interaction increases SREBP-1c and AMPK activity.

**Conclusions**—This study provides evidence for a role of RTN3 in inducing obesity and TG accumulation, and suggests that inhibiting the expression of RTN3 in fat tissue may be a novel therapeutic approach to treat obesity and hypertriglyceridemia.

\*Correspondence: Rong Xiang, PH.D: Fax number: +86073182650230; Telephone number: +86073182650230, shirlesmile@csu.edu.cn; School of Life Sciences, Central South University, Changsha, People's Republic of China, Or Kun Xia, PH.D, Fax number: +86073182650230; Telephone number: +86073182650230, xiakun@sklmg.edu.cn, School of Life Sciences, Central South University, Changsha, People's Republic of China.

#Dr. Xiang, Dr. Fan, Dr. Huang and Dr. Chen contributed equally to this study.

### Conflicts of interest

The authors have no conflicts of interest to declare.

## Keywords

RTN3; obesity; hypertriglyceridemia; lipid droplets; HSPA5

---

## Introduction

Obesity and its comorbidities such as heart disease, diabetes, and certain types of cancers contribute to mostly-preventable deaths both in adults and children. The increasing rates of these health issues are the most serious and arduous public health challenge of the 21st century<sup>1</sup>. Although many possible contributors and mediators involved in the development and maintenance of obesity have been reported in recent years<sup>2-4</sup>, mechanistic links to these factors remained to be fully established. Among these factors, triglycerides (TGs) and TG metabolism are linked to the occurrence of obesity and many obesity-related diseases. TG is neutral fat that is mostly stored in lipid droplets (LDs), which are defined as the major fat storage organelles in eukaryotes<sup>5, 6</sup>. Human adipocytes are the most highly-specialized cell type and can store vast quantity of energy in LDs, primarily as TGs. To accommodate more TGs, adipocytes frequently form new LDs and expand existing ones, increasing the TG storage and LD capacity in the adipose tissue, which is the major mechanism of obesity in adults<sup>7-9</sup>.

The reticulon (RTN) protein family consists of RTN1 to RTN4 in mammalian systems and has a signature C-terminal RTN homolog domain (RHD)<sup>10, 11</sup>. Biochemically, RTNs have been shown to shape tubular endoplasmic reticulum (ER) structure due to the presence of a  $\omega$ - (wedge-shaped) membrane topology in which both the N- and C-terminal domains face the cytosolic side<sup>12, 13</sup>. Functionally, RTNs have been found to regulate neurite outgrowth<sup>14</sup>, to negatively modulate the activity of Alzheimer's  $\beta$ -secretase<sup>15, 16</sup>, and to pathologically link to axonopathy in hereditary spastic paraplegias<sup>17</sup>. Interestingly, the functions of RTNs in human peripheral organs remain underexplored. For example, it has not been established whether RTN3 expression has any effects on obesity and/or TG metabolism.

To this end, we noted an obesity phenotype and abnormal accumulation of TGs in the plasma and fat tissue of transgenic mice overexpressing the wild-type human RTN3 gene (Tg-RTN3). We then collected fat tissue from obese individuals and normal-weight, age-matched controls, as well as plasma samples of patients with hypertriglyceridemia and controls. Strikingly, high expression of human RTN3 (hRTN3) is associated with obesity and high levels of TGs in fat tissue and plasma. To further establish whether RTN3 contributes to elevated TG concentration in plasma and fat tissue, we examined RTN3-null mice. We showed that RTN3-null mice that were fed with high-fat diet displayed a TG accumulation barrier. Also, overexpressing the reticulon homologous gene (*ret-1*) in *C. elegans* increased the number and size of large LDs. Conversely, knocking down the expression of *ret-1* reduced the number and size of large LDs in *C. elegans* lacking *daf-22*, which further indicates a role of RTN3 in TG accumulation. Our mechanistic study revealed that RTN3 interacts with heat shock protein family A (Hsp70) member 5 (HSPA5) and regulates the activation of SREBP-1c and AMPK, which are two important downstream molecules in TG biosynthesis. Thus, our findings suggest that RTN3 may contribute to obesity and

hypertriglyceridemia, possibly by modifying TG synthesis and LD size expansion. Furthermore, elevated RTN3 in plasma may indicate an increased risk of obesity.

## Methods

The data, analytic methods, and study materials will not be made available to other researchers for purposes of reproducing the results or replicating the procedure.

### Mouse strains, cell lines, human tissues samples and reagents

Tg-RTN3 mice and RTN3-null mice were generated and genotyping was performed as described previously<sup>16, 18, 19</sup>. 3T3L1 pre-adipocytes were purchased from the Cell Bank of Shanghai Institutes for Biological Sciences (Shanghai, China) and maintained at 37°C in a humidified, 5% CO<sub>2</sub>-controlled atmosphere in Dulbecco's modified Eagle's medium (DMEM) supplemented with 10% fetal bovine serum, 50 IU/ml penicillin, 50 mM streptomycin, and glutamine.

The study protocol was approved by the Review Board of the Central South University in China. All human subjects were enrolled from the Second Xiangya Hospital of Central South University. Fat tissue was collected from liposuction patients and control fat tissue was collected from surgical operations on patients with congenital heart defects. All patients provided written informed consent.

RTN1-4 antibody was generated in the Yan laboratory<sup>20</sup>. HSPA5, SCAP, SREBP-1c, AMPK, p-AMPK and GAPDH antibodies were purchased from Cell Signaling Technology (CST). BODIPY and Nile Red dye were purchased from Thermo Fisher. The control diet was purchased from Shanghai SLAC Laboratory Animal Co., Ltd. High-fat diet was purchased from TROPHIC Animal Feed High-Tech Co., Ltd., China and consisted of 60% fat, 20% protein, and 20% carbohydrate.

### *C. elegans* strains and transgenes

Nematode growth media (NGM) was used to maintain *Caenorhabditis elegans* (*C. elegans*) with OP50 *Escherichia coli* at 20°C<sup>21</sup>. The wild-type strain was N2 (Bristol) and the mutant strain used in this study was *daf-22* (ok693)<sup>22</sup>.

Germline transgene experiments were performed as described previously<sup>23</sup>. Transgene mixtures contained 10 ng/μl pPD95.79::ret-1p::ret-1 and 20 ng/μl pPD95.86::GFP (*myo-3p::GFP*) plasmid (which expresses GFP in body-wall muscles) as a co-injection marker.

### RNAi screening

Young adult *C. elegans* were fed with HT115 (DE3) bacteria containing plasmids expressing dsRNAs targeting *ret-1* on NGM plates with 1 mM IPTG and 0.1 mg/ml Ampicillin for 2 days.

### Co-IP and Western blot analyses

For Western blotting, fat tissue and liver tissue were homogenized on ice in 1% CHAPS extraction buffer containing complete protease inhibitors (Roche Bioscience, #04693159001) and 0.1 mM Na<sub>3</sub>VO<sub>4</sub> for inhibiting phosphatase. The homogenates were rotated for 30 min at 4°C to ensure extraction of membrane proteins. After centrifugation at 15,000×g for 120 min, supernatants were collected and protein concentration was measured with the BCA protein assay reagent (Pierce). Equal amounts of protein lysates were resolved on 4-12% Bis-Tris NuPAGE gels, followed by standard Western blotting with the antibodies specified above. Chemiluminescent signals were scanned and integrated density values were calculated with a chemiluminescent imaging system (Alpha Innotech).

For Co-IP, 3T3L1 cells were first grown in DMEM for 24 h in 60-mm plates to ~ 80% confluence and then transfected with the indicated expression constructs. After being cultured for 48 h, cells were lysed and equal amounts of lysates (500 µg in 1 ml) were used for immunoprecipitation with Myc or Flag-conjugated beads overnight. The extensively-washed immunoprecipitates were resolved on a 4-12% NuPage Bis-Tris gel, followed by standard Western blotting with the antibodies specified above. Chemiluminescent signals were scanned and integrated density values were calculated with a chemiluminescent imaging system (Alpha Innotech).

### Immunofluorescent confocal microscopy

BODIPY and Nile Red vital staining in live animals were essentially the same as described previously<sup>24</sup>. For BODIPY staining, 500 µl of 5 µM C1-BODIPY-C12 (Invitrogen) in M9 buffer was added on to a 60-mm NGM plate. For Nile Red staining, 100 µl of 5 µg/mL Nile Red (Invitrogen) in M9 buffer was added onto a 60-mm NGM plate. The plates were immediately dried in a laminar flow hood and were used to grow and stain nematodes. *C. elegans* were fixed in 4% paraformaldehyde on slides. After washed by PBS, slides were checked by confocal microscopy.

### Hematoxylin-eosin (H&E) staining

Paraformaldehyde-fixed fat tissue was embedded in paraffin and sliced into 6 µm sections. The sections were stained with H&E and examined by routine light microscopy (Olympus Corporation, Tokyo, Japan). Briefly, sections were dried, followed by xylene dewaxing and rehydration with decreasing concentrations of alcohol. The slides were then stained with hematoxylin for 15 min and differentiated with hydrochloric acid alcohol for 30 sec. Following staining with 1% ammonia, sections were stained with 1% eosin for 2 min, followed by dehydration in alcohol and mounting.

### Immunohistochemistry

Immunohistochemistry experiments were performed using a Histostain-Plus Kit (Maibio, Shanghai, China). Liver tissue from mice was sectioned in the sagittal plane at a thickness of 10 µm using a cryostat after 4% paraformaldehyde fixation and optimal cutting temperature compound embedding.

## Statistical analysis

Data were subjected to statistical analysis with Graph-Pad Prism 5 (GraphPad Software) and were plotted by AI Illustrator (Adobe). Results represent the mean  $\pm$  SEM of at least 3 independent experiments as indicated in the figure legends. Two-tailed Student's t-tests based on ANOVA were used for two-group comparisons. For multiple comparisons, we conducted one-way ANOVAs with Dunnett's correction to analyze differences among the control group and one or more independent treatment groups. Differences were considered statistically significant at  $P < 0.05$ , with significance indicated in figures as \* $P < 0.05$ , \*\* $P < 0.01$ , \*\*\* $P < 0.001$ . NS represents no significant difference.

## Results

### ***Rtn3* transgenic mice exhibit a phenotype related to obesity and hypertriglyceridemia**

Transgenic mice overexpressing RTN3 (Tg-RTN3 mice) were previously generated to investigate the role of RTN3 in the regulation of Beta-Secretase 1 (BACE1) activity and in the formation of dystrophic neurites<sup>16, 18, 24</sup>. However, it was also noted that Tg-RTN3 mice exhibited larger body size compared to WT controls (Figure 1A). This higher body weight was prominent at four months of age with standard chow, with the average body weight of Tg-RTN3 mice being ~45.03% higher compared to WT control littermates (Figure 1B). It was noticeable that the epididymis adipose tissues accumulated in Tg-RTN3 mice was approximately 284% greater than that in WT littermates (Figure 1C). Although the RTN3 transgene was targeted by prion-promoter for neuronal expression<sup>11</sup>, we showed that RTN3 was also expressed in fat tissue, as the expression of RTN3 transgene was visibly higher than that of WT (Figure 1D-E, Figure S1). Plasma TG levels in Tg-RTN3 mice were obviously increased compared to WT control littermates after 16 weeks of standard chow. The level of plasma TG in Tg-RTN3 mice was increased to approximately 188% compared to that in WT controls (Figure 1F). Thus, increased expression of RTN3 resulted in elevated levels of TG in the plasma and fat tissue.

To further determine whether the accumulation of TG alters LD size, we conducted H&E staining to analyze the size of fat cells in Tg-RTN3 and WT control mice. We found that the sizes of fat cells in Tg-RTN3 mice were visibly and statistically larger than those in WT control mice (Figure 1G-H). We also found that the TG levels of adipose tissue in Tg-RTN3 mice were higher than in WT controls (Figure 1I). These observations in Tg-RTN3 mice suggests that increased overexpression of RTN3 is sufficient to cause adipose tissue expansion by increasing the size of LDs in adipocytes and elevating TG levels in the plasma.

### **The link between high RTN3 expression and obesity/hypertriglyceridemia in human**

In obesity patients (Body Mass Index>28), the size of LDs is also frequently larger than that in non-obese individuals (Figure 2A-B). We therefore further explored the relationship between the expression of RTN3 and obesity. In order to test the hypothesis that RTN3 participates in LD expansion and TG accumulation in human, we collected adipose biopsy samples from obese individuals and normal body weight controls (BMI<23.7). By western blot analysis, we found that RTN3 levels were evidently higher in individuals with obesity (n=4) than those in the normal body weight (n=3) controls (see examples in Figure 2C-D).

Furthermore, we collected peripheral blood samples (leukocytes) from individuals with obesity and/or hypertriglyceridemia ( $TG > 2.83$  mmol/L). A total of 149 obesity patients, 343 hypertriglyceridemia patients, and 84 healthy controls ( $18.5 < BMI < 22.9$ ,  $TG < 1.7$  mmol/L) were enrolled in this study (Table 1). The mean plasma TG values of these three groups were  $11.26 \pm 4.90$  mmol/L,  $7.82 \pm 5.17$  mmol/L, and  $1.05 \pm 0.80$  mmol/L, respectively. There are 71 hypertriglyceridemia patients and 19 obesity patients had a history of coronary heart disease (CHD) and/or atherosclerosis (AS) (Table 1). Western blot analysis of protein lysates from each individual's leukocyte were conducted. We found that 32.65% (112/343) of hypertriglyceridemia patients (upper cluster) and 35.57% (53/149) of obesity patients (upper cluster) exhibited higher RTN3 levels compared to healthy controls ( $n=86$ ), which were arbitrarily set as 1 for most representative cases (Figure 2E). In addition, we also collected some fat tissue from hypertriglyceridemia patients ( $n=12$ ) and healthy controls ( $n=2$ ). Western blot analyses showed that the RTN3 levels in three hypertriglyceridemia patients' samples were much higher than those in healthy controls (Figure 2F-G). These findings indicate that RTN3 levels are elevated in obesity and hypertriglyceridemia patients. All of these human data were consistent with our findings in the Tg-RTN3 mouse model.

### **RTN3 deficiency leads to resistance against TG accumulation following a high-fat diet**

Since overexpression of RTN3 in mice can expand the size of LDs and increase plasma TG levels, we then explored whether RTN3 deficiency would decrease LD size and TG accumulation in mouse model. We generated RTN3 homozygous knockout (RTN3 KO) mice utilizing CRISPR technology (Figure 3A). Contrary to our initial expectation, there were no obvious difference between RTN3 KO mice and WT mice in any age group (Figure S2), suggesting that RTN3 deficiency has no obvious effect on adipose tissue accumulation during normal growth.

We next assessed whether RTN3 deficiency would affect LD size and/or TG levels under stressed conditions such as high-fat diet (HFD), which is one of the major approaches to induce TG accumulation. In our experiment, mice were fed with HFD daily beginning at 8 weeks of age for 21 weeks. After 21 weeks of continuous HFD, WT mice exhibited visibly larger body size compared to RTN3 KO mice (Figure 3B). The body weight of HFD WT mice at the age of 22 weeks on average was  $46.23 \pm 1.86$ g, compared to  $35.74 \pm 1.15$  g in HFD RTN3 KO mice (Figure 3C).

We also examined fat tissue directly after HFD, and found that RTN3 KO mice displayed diminished adipose tissue depots, with 39.3% reduction in white fat pad mass of epididymis compared to WT controls (Figure 3D). The levels of plasma TGs in HFD WT mice were much higher than those in normal diet WT mice (Figure 1F, Figure 3E). Remarkably, the levels of TGs in RTN3 KO mice after HFD were lower compared to those in HFD WT mice (Figure 3E).

In addition, H&E staining revealed a smaller size of fat cells in RTN3 KO mice compared to that in WT control littermates after 21 weeks of HFD (Figure 3F-G). Also, the TG levels in adipose tissue in HFD RTN3 KO mice were lower than that in HFD WT controls (Figure 3H). These data collectively indicate that the deletion of RTN3 in mice decreases TG accumulation in plasma, as well as LD accumulation in fat tissue.

### RET-1 is required for LD expansion and TG accumulation in *C. elegans*

*C. elegans* is an ideal animal model in LD research. In *C. elegans*, *ret-1* is the only *rtn* gene and it has high homology to mammalian *RTN3*. In order to understand the effect of *RTN3* on LD size, we altered the expression of *ret-1* in *C. elegans* and monitored LD size with BODIPY and TG levels with Nile Red. To better analyze LD size in *C. elegans*, we first generated overexpressing *ret-1* *C. elegans* by plasmid injection (Figure S3). Large LD size (diameter >3  $\mu\text{m}$ ) or average LD size and TG levels were significantly increased in this group (Figure 4A-D).

A previous study demonstrated that excess TGs in expanded LDs would be accumulated in *C. elegans* lacking *daf-22*, which is the terminal thiolase for peroxisomal fatty acid  $\beta$  oxidation<sup>21</sup>. In WT background, *ret-1* is not required for LD formation, but participates in TG accumulation. We then conducted suppressed expression of *ret-1* by siRNA silencing in a *daf-22* mutant background. The results indicated that knocking down *ret-1* expression suppressed LD expansion and reduced TG levels (Figure 4A-D). All of these results in *C. elegans* suggest that *ret-1* is required for LD expansion and TG accumulation. They also indicate that *RTN3* may be a mammalian *RTN* gene conserved for the control of LD expansion and TG accumulation.

### Increased *RTN3* can bind HSPA5 and activate SREBP-1c and AMPK

To explore the underlying mechanism of elevated *RTN3* in regulating LD size and TG accumulation, we explored *RTN3*-interacting proteins in Tg-*RTN3* mouse fat tissue by co-immunoprecipitation (co-IP) and mass spectrometric analyses (MS). HSPA5 was identified as a *RTN3*-interacting protein (data not shown). This protein-to-protein interaction was further validated by co-IP experiments in 3T3L1 cells (Figure 5A, Figure S4). HSPA5, also known as BIP/GRP78, is an ER chaperone facilitating a wide range of protein folding processes<sup>25, 26</sup>. Relevant to our study, HSPA5 has been shown to participate in the formation of a complex containing sterol regulatory element-binding protein (SREBP) and SREBP cleavage-activating protein (SCAP) by stabilizing SREBP-SCAP complex substance<sup>27, 28</sup>. HSPA5 has also been shown to regulate the activation of SREBP-1c, which is a key transcription factor in promoting TG lipid synthesis<sup>25, 29</sup>.

The discovery of *RTN3* and HSPA5 interaction raised the question as to whether elevated *RTN3* can increase binding to HSPA5 and further sequester HSPA5 physiological function. To address this question, we altered *RTN3* expression in the 3T3L1 cell line by siRNA knock-down or *RTN3* overexpression. Our results showed that the total levels of HSPA5 were unaffected by altered *RTN3* levels (Figure 5B-C). However, co-IPed HSPA5 was significantly greater in the Tg-*RTN3* model than in WT or the siRNA-*RTN3* model (Figure 5B-C). This increased interaction appeared to increase the levels of SCAP and activated SREBP-1c in the Tg-*RTN3* model (Figure 5B-C). Immunohistochemistry staining further confirmed that expression levels of SREBP-1c in Tg-*RTN3* mouse liver tissue were higher than those in WT mice (Figure 5D-E). In HFD *RTN3* KO mouse livers, SREBP-1c expression levels were lower than in HFD WT mice (Figure 5F-G).

In addition, to determine whether increased RTN3 induces LD expansion via interactions with HSPA5 and further regulates SREBP-1c expression, we knocked down the homologous genes of *HSPA5* (*hsp-4*) and *SREBP-1c* (*sbp-1*) in *C. elegans* overexpressing *ret-1*. We showed that knocking down *hsp4* may induce the LD expansion, but knocking down *sbp-1* suppressed LD expansion (Figure 5H-I). These results suggest that increased RTN3 activates SREBP-1c by competitively binding to HSPA5. In return, SREBP-1c can further regulate the levels of TG synthesis by inducing the activation of AMPK<sup>30, 31</sup>. We found that the levels of AMPK in Wt, Tg-RTN3, HFD Wt and HFD RTN3 KO groups are similar (Figure 5J-K). However, Tg-RTN3 mice exhibited higher levels of p-AMPK than WT mice (Figure 5J-K). Consistent with these findings, levels of p-AMPK in HFD-treated WT mice were higher than those in HFD RTN3 KO mice (Figure 5J-K). Collectively, our data showed that with increased availability of RTN3, more HSPA5 will bind to RTN3 instead of the SREBP1-SCAP complex, consequently resulting in SREBP-1c activation, which plays a critical role in regulating TG levels and LD size.

## Discussion

RTN3 is an ER membrane protein that appears to exert various biological functions such as modulating A $\beta$  levels, apoptosis, and autophagic responses<sup>20, 32–35</sup>. However, this protein is broadly expressed and has multiple spliced variants<sup>16</sup>. Whether this tubular ER-related protein is involved in lipid-related health and disease has never been revealed. In this study, we provided clinical and genetic evidence that the enhanced expression of RTN3 in fat tissue potentially leads to TG accumulation and obesity. Our results may suggest a causative relationship between increased RTN3 and obesity or hypertriglyceridemia in patients.

The mechanism underlying how increased expression of RTN3 leads to obesity and TG accumulation merits need further exploration. In this study, we identified HSPA5 as a novel RTN3-interacting protein. The activity of HSPA5 is crucial in regulating TG accumulation and LD expansion. Lipid synthesis in mammalian cells is controlled by SREBPs, which are ER membrane-bound proteins. SREBP transcriptional activity is regulated through proteolytic cleavage at a leucine residue by S1P to release SREBP-1c<sup>26, 28, 36</sup>. When SREBP forms a complex with SCAP, proteolytic cleavage activity is suppressed. HSPA5 is a protein that is important for maintaining the stability of the SREBP-SCAP complex substance to suppress S1P cleavage and lipid biosynthesis<sup>25, 27</sup>. In our study, we showed that the increased expression of RTN3 can facilitate interactions between RTN3 and HSPA5, thereby decreasing the activity of HSPA5 in stabilizing the SREBP-SCAP complex. Subsequently, the levels of free SCAP increased and eventually activated S1P to cleave SREBPS to form SREBP-1c (Figure 6). Consistent with these results, we also found that competitive binding and activation of SREBP-1c induced LD expansion in *C. elegans*. Moreover, we confirmed that p-AMPK, which is the downstream pathway of TG accumulation, was also significantly increased in fat tissue of Tg-RTN3 mice and was higher in HFD WT mice than in HFD RTN3-null mice.

The theory that LDs emerge from the tubular ER is supported by results from various models for LD biogenesis<sup>37</sup>. Our findings are consistent with a previous report in which *C. elegans* was used as the model organism to identify genes that are important for the control



of LD size<sup>38</sup>. In this unbiased screening assay, tubular ER-related proteins such as REEP2, REEP5, and atlastin were found to regulate LD size in the *C. elegans* model<sup>21, 22</sup>. Here, we demonstrate that RTN3 plays an important role in the regulation of LD size, as RTN3 deficiency is sufficient to mediate changes in LD size.

Many enzymes involved in neutral lipid synthesis are localized in the ER, suggesting a role for tubular ER proteins in the generation and expansion of LDs<sup>39</sup>. For example, neutral lipid synthesizing enzymes such as DGAT1 and phospholipid synthesizing enzymes such as CPT are localized in the ER<sup>40</sup>. Fat storage-inducing transmembrane proteins are part of the evolutionarily-conserved FIT protein family, which reside in the ER. Overexpression of either FIT1 or FIT2 in mammalian cells results in the accumulation of LDs in skeletal muscle or murine liver in culture or *in vivo*<sup>41</sup>. It is likely that the physical link between tubular ER and LDs plays a critical role in the regulation of LD size.

Interestingly, we found that increased expression of RTN3 will not only expand LD size, but will also cause accumulation of TGs. We revealed that plasma RTN3 was increased in hypertriglyceridemia patients in addition to individuals with obesity. The accumulation of TGs and the expansion of LD sizes were both observed in Tg-RTN3 mice and *ret-1* overexpression *C. elegans*. This study provides evidence that RTN3 not only regulates TG accumulation in plasma and fat tissue, but also participates in LD expansion.

Among the RTN family, the C-terminal domains of the four members have a reticulon homology domain (RHD) with similar functions<sup>10</sup>. It has been demonstrated that RTNs can form a homodimer or a heterodimer and activate different downstream signaling pathways. Over-expression of RTN3 or RTN4 has been shown to induce cell apoptosis in cultured cells<sup>33, 35</sup>. However, we did not find any association between obesity or TG elevation with other RTN members, indicating a distinctive role of RTN3 in dyslipidemia and obesity among the RTN family.

In summary, our study suggests that Tg-RTN3 mice might be an ideal model for research on obesity and hypertriglyceridemia, as the model recapitulates the features of obesity. Increased RTN3 expression is a potential risk factor for excessive TG storage in fat cells by expanding LD size, partly through competitive binding on HSPA5 to activate SREBP-1c and AMPK. Hence, our findings shed light on the importance of the relationship between ER proteins and obesity or hypertriglyceridemia in humans and animals. Collectively, our data suggest that RTN3 is a key molecule in lipid metabolism.

## Supplementary Material

Refer to Web version on PubMed Central for supplementary material.

## Acknowledgments

We thank the patients and their families for participating in this study. We thank Prof. Long Ma, Prof. Jia-da Li, and Bei-bei Cao from the School of Life Sciences, Central South University for *C. elegans* and mouse-related technical assistance.

## Sources of Funding

This study was supported by the National Natural Science Foundation of China (81370394), the National Basic Research Program of China (973 Program) (2012CB517900) and National Institute of Aging (R01AG025493).

## References

1. Swinburn BA, Sacks G, Hall KD, McPherson K, Finegood DT, Moodie ML, Gortmaker SL. The global obesity pandemic: Shaped by global drivers and local environments. *Lancet*. 2011; 378:804–814. DOI: 10.1016/S0140-6736(11)60813-1 [PubMed: 21872749]
2. Cui J, Ding Y, Chen S, Zhu X, Wu Y, Zhang M, Zhao Y, Li TR, Sun LV, Zhao S, Zhuang Y, Jia W, Xue L, Han M, Xu T, Wu X. Disruption of gpr45 causes reduced hypothalamic pomc expression and obesity. *J Clin Invest*. 2016; 126:3192–3206. DOI: 10.1172/JCI85676 [PubMed: 27500489]
3. Li J, Song J, Zaytseva YY, Liu Y, Rychahou P, Jiang K, Starr ME, Kim JT, Harris JW, Yiannikouris FB, Katz WS, Nilsson PM, Orho-Melander M, Chen J, Zhu H, Fahrenholz T, Higashi RM, Gao T, Morris AJ, Cassis LA, Fan TW, Weiss HL, Dobner PR, Melander O, Jia J, Evers BM. An obligatory role for neurotensin in high-fat-diet-induced obesity. *Nature*. 2016; 533:411–415. DOI: 10.1038/nature17662 [PubMed: 27193687]
4. Lynch L, Hogan AE, Duquette D, Lester C, Banks A, LeClair K, Cohen DE, Ghosh A, Lu B, Corrigan M, Stevanovic D, Maratos-Flier E, Drucker DJ, O’Shea D, Brenner M. Ink cells induce fgf21 for thermogenesis and are required for maximal weight loss in glp1 therapy. *Cell Metab*. 2016; 24:510–519. DOI: 10.1016/j.cmet.2016.08.003 [PubMed: 27593966]
5. Vega-Lopez S, Calle MC, Fernandez ML, Kollanoor-Samuel G, Chhabra J, Todd M, Segura-Perez S, D’Agostino D, Damio G, Perez-Escamilla R. Triglyceride screening may improve cardiometabolic disease risk assessment in latinos with poorly controlled type 2 diabetes. *J Health Care Poor Underserved*. 2013; 24:1739–1755. DOI: 10.1353/hpu.2013.0171 [PubMed: 24185167]
6. Sacks FM, Carey VJ, Anderson CA, Miller ER 3rd, Copeland T, Charleston J, Harshfield BJ, Laranjo N, McCarron P, Swain J, White K, Yee K, Appel LJ. Effects of high vs low glycemic index of dietary carbohydrate on cardiovascular disease risk factors and insulin sensitivity: The omniscarb randomized clinical trial. *JAMA*. 2014; 312:2531–2541. DOI: 10.1001/jama.2014.16658 [PubMed: 25514303]
7. Hashimoto T, Yokokawa T, Endo Y, Iwanaka N, Higashida K, Taguchi S. Modest hypoxia significantly reduces triglyceride content and lipid droplet size in 3t3-l1 adipocytes. *Biochem Biophys Res Commun*. 2013; 440:43–49. DOI: 10.1016/j.bbrc.2013.09.034 [PubMed: 24041687]
8. Rizzatti V, Boschi F, Pedrotti M, Zoico E, Sbarbati A, Zamboni M. Lipid droplets characterization in adipocyte differentiated 3t3-l1 cells: Size and optical density distribution. *Eur J Histochem*. 2013; 57:159–162. DOI: 10.4081/ejh.2013.e24
9. Boschi F, Rizzatti V, Zamboni M, Sbarbati A. Simulating the dynamics of lipid droplets in adipocyte differentiation. *Comput Methods Programs Biomed*. 2017; 138:65–71. DOI: 10.1016/j.cmpb.2016.10.013 [PubMed: 27886716]
10. Oertle T, Klinger M, Stuermer CA, Schwab ME. A reticular rhapsody: Phylogenetic evolution and nomenclature of the rtn/nogo gene family. *FASEB J*. 2003; 17:1238–1247. DOI: 10.1096/fj.02-1166hyp [PubMed: 12832288]
11. Yan R, Shi Q, Hu X, Zhou X. Reticulon proteins: Emerging players in neurodegenerative diseases. *Cell Mol Life Sci*. 2006; 63:877–889. DOI: 10.1007/s00018-005-5338-2 [PubMed: 16505974]
12. Voeltz GK, Prinz WA, Shibata Y, Rist JM, Rapoport TA. A class of membrane proteins shaping the tubular endoplasmic reticulum. *Cell*. 2006; 124:573–586. DOI: 10.1016/j.cell.2005.11.047 [PubMed: 16469703]
13. He W, Shi Q, Hu X, Yan R. The membrane topology of rtn3 and its effect on binding of rtn3 to bace1. *J Biol Chem*. 2007; 282:29144–29151. DOI: 10.1074/jbc.M704181200 [PubMed: 17699523]
14. Schwab ME, Strittmatter SM. Nogo limits neural plasticity and recovery from injury. *Curr Opin Neurobiol*. 2014; 27:53–60. DOI: 10.1016/j.conb.2014.02.011 [PubMed: 24632308]
15. Prior M, Shi Q, Hu X, He W, Levey A, Yan R. Rtn/nogo in forming alzheimer’s neuritic plaques. *Neurosci Biobehav Rev*. 2010; 34:1201–1206. DOI: 10.1016/j.neubiorev.2010.01.017 [PubMed: 20144652]

16. Sharoar MG, Shi Q, Ge Y, He W, Hu X, Perry G, Zhu X, Yan R. Dysfunctional tubular endoplasmic reticulum constitutes a pathological feature of alzheimer's disease. *Mol Psychiatry*. 2016; 21:1263–1271. DOI: 10.1038/mp.2015.181 [PubMed: 26619807]
17. Renvoise B, Blackstone C. Emerging themes of er organization in the development and maintenance of axons. *Curr Opin Neurobiol*. 2010; 20:531–537. DOI: 10.1016/j.conb.2010.07.001 [PubMed: 20678923]
18. Hu X, Shi Q, Zhou X, He W, Yi H, Yin X, Gearing M, Levey A, Yan R. Transgenic mice overexpressing reticulon 3 develop neuritic abnormalities. *EMBO J*. 2007; 26:2755–2767. DOI: 10.1038/sj.emboj.7601707 [PubMed: 17476306]
19. Shi Q, Ge Y, Sharoar MG, He W, Xiang R, Zhang Z, Hu X, Yan R. Impact of rtn3 deficiency on expression of bace1 and amyloid deposition. *J Neurosci*. 2014; 34:13954–13962. DOI: 10.1523/JNEUROSCI.1588-14.2014 [PubMed: 25319692]
20. He W, Lu Y, Qahwash I, Hu XY, Chang A, Yan R. Reticulon family members modulate bace1 activity and amyloid-beta peptide generation. *Nat Med*. 2004; 10:959–965. DOI: 10.1038/nm1088 [PubMed: 15286784]
21. Xu N, Zhang SO, Cole RA, McKinney SA, Guo F, Haas JT, Bobba S, Farese RV Jr, Mak HY. The fatp1-dgat2 complex facilitates lipid droplet expansion at the er-lipid droplet interface. *J Cell Biol*. 2012; 198:895–911. DOI: 10.1083/jcb.201201139 [PubMed: 22927462]
22. Klemm RW, Norton JP, Cole RA, Li CS, Park SH, Crane MM, Li L, Jin D, Boye-Doe A, Liu TY, Shibata Y, Lu H, Rapoport TA, Farese RV Jr, Blackstone C, Guo Y, Mak HY. A conserved role for atlastin gtpases in regulating lipid droplet size. *Cell Rep*. 2013; 3:1465–1475. DOI: 10.1016/j.celrep.2013.04.015 [PubMed: 23684613]
23. Mello CC, Kramer JM, Stinchcomb D, Ambros V. Efficient gene transfer in c.Elegans: Extrachromosomal maintenance and integration of transforming sequences. *EMBO J*. 1991; 10:3959–3970. [PubMed: 1935914]
24. Shi Q, Hu X, Prior M, Yan R. The occurrence of aging-dependent reticulon 3 immunoreactive dystrophic neurites decreases cognitive function. *J Neurosci*. 2009; 29:5108–5115. DOI: 10.1523/JNEUROSCI.5887-08.2009 [PubMed: 19386906]
25. Kammoun HL, Chabanon H, Hainault I, Luquet S, Magnan C, Koike T, Ferre P, Foufelle F. Grp78 expression inhibits insulin and er stress-induced srebp-1c activation and reduces hepatic steatosis in mice. *J Clin Invest*. 2009; 119:1201–1215. DOI: 10.1172/JCI37007 [PubMed: 19363290]
26. Wang J, Sevier CS. Formation and reversibility of bip protein cysteine oxidation facilitate cell survival during and post oxidative stress. *J Biol Chem*. 2016; 291:7541–7557. DOI: 10.1074/jbc.M115.694810 [PubMed: 26865632]
27. Misra UK, Pizzo SV. Activated alpha2-macroglobulin binding to human prostate cancer cells triggers insulin-like responses. *J Biol Chem*. 2015; 290:9571–9587. DOI: 10.1074/jbc.M114.617837 [PubMed: 25720493]
28. Ji C, Chan C, Kaplowitz N. Predominant role of sterol response element binding proteins (srebp) lipogenic pathways in hepatic steatosis in the murine intragastric ethanol feeding model. *J Hepatol*. 2006; 45:717–724. DOI: 10.1016/j.jhep.2006.05.009 [PubMed: 16879892]
29. Fang DL, Wan Y, Shen W, Cao J, Sun ZX, Yu HH, Zhang Q, Cheng WH, Chen J, Ning B. Endoplasmic reticulum stress leads to lipid accumulation through upregulation of srebp-1c in normal hepatic and hepatoma cells. *Mol Cell Biochem*. 2013; 381:127–137. DOI: 10.1007/s11010-013-1694-7 [PubMed: 23703028]
30. Tajima-Shirasaki N, Ishii KA, Takayama H, Shirasaki T, Iwama H, Chikamoto K, Saito Y, Iwasaki Y, Teraguchi A, Lan F, Kikuchi A, Takeshita Y, Muraio K, Matsugo S, Kaneko S, Misu H, Takamura T. Eicosapentaenoic acid down-regulates expression of the selenoprotein p gene by inhibiting srebp-1c protein independently of the amp-activated protein kinase pathway in h4iiec3 hepatocytes. *J Biol Chem*. 2017; 292:10791–10800. DOI: 10.1074/jbc.M116.747006 [PubMed: 28465347]
31. Wang S, Li X, Guo H, Yuan Z, Wang T, Zhang L, Jiang Z. Emodin alleviates hepatic steatosis by inhibiting sterol regulatory element binding protein 1 activity by way of the calcium/calmodulin-dependent kinase kinase-amp-activated protein kinase-mechanistic target of rapamycin-p70 ribosomal s6 kinase signaling pathway. *Hepatol Res*. 2016; 47:683–701. DOI: 10.1111/hepr.12788 [PubMed: 27492505]

32. Mungai PT, Waypa GB, Jairaman A, Prakriya M, Dokic D, Ball MK, Schumacker PT. Hypoxia triggers ampk activation through reactive oxygen species-mediated activation of calcium release-activated calcium channels. *Mol Cell Biol.* 2011; 31:3531–3545. DOI: 10.1128/MCB.05124-11 [PubMed: 21670147]
33. Zhu L, Xiang R, Dong W, Liu Y, Qi Y. Anti-apoptotic activity of bcl-2 is enhanced by its interaction with rtn3. *Cell Biol Int.* 2007; 31:825–830. DOI: 10.1016/j.cellbi.2007.01.032 [PubMed: 17379544]
34. Lee JT, Lee TJ, Kim CH, Kim NS, Kwon TK. Over-expression of reticulon 3 (rtn3) enhances trail-mediated apoptosis via up-regulation of death receptor 5 (dr5) and down-regulation of c-flip. *Cancer Lett.* 2009; 279:185–192. DOI: 10.1016/j.canlet.2009.01.035 [PubMed: 19250737]
35. Chen Y, Zhao S, Xiang R. Rtn3 and rtn4: Candidate modulators in vascular cell apoptosis and atherosclerosis. *J Cell Biochem.* 2010; 111:797–800. DOI: 10.1002/jcb.22838 [PubMed: 20717916]
36. Gong X, Qian H, Shao W, Li J, Wu J, Liu JJ, Li W, Wang HW, Espenshade P, Yan N. Complex structure of the fission yeast srebp-scrap binding domains reveals an oligomeric organization. *Cell Res.* 2016; 26:1197–1211. DOI: 10.1038/cr.2016.123 [PubMed: 27811944]
37. Wang CW. Lipid droplets, lipophagy, and beyond. *Biochim Biophys Acta.* 2016; 1861:793–805. DOI: 10.1016/j.bbali.2015.12.010 [PubMed: 26713677]
38. Zhang SO, Box AC, Xu N, Le Men J, Yu J, Guo F, Trimble R, Mak HY. Genetic and dietary regulation of lipid droplet expansion in *caenorhabditis elegans*. *Proc Natl Acad Sci U S A.* 2010; 107:4640–4645. DOI: 10.1073/pnas.0912308107 [PubMed: 20176933]
39. Yen CL, Stone SJ, Koliwad S, Harris C, Farese RV Jr. Thematic review series: Glycerolipids. Dgat enzymes and triacylglycerol biosynthesis. *J Lipid Res.* 2008; 49:2283–2301. DOI: 10.1194/jlr.R800018-JLR200 [PubMed: 18757836]
40. Wilfling F, Haas JT, Walther TC, Farese RV Jr. Lipid droplet biogenesis. *Curr Opin Cell Biol.* 2014; 29:39–45. DOI: 10.1016/j.ceb.2014.03.008 [PubMed: 24736091]
41. Gross DA, Zhan C, Silver DL. Direct binding of triglyceride to fat storage-inducing transmembrane proteins 1 and 2 is important for lipid droplet formation. *Proc Natl Acad Sci U S A.* 2011; 108:19581–19586. DOI: 10.1073/pnas.1110817108 [PubMed: 22106267]

### Clinical Perspective

#### What is new?

- We established a linkage between Reticulon 3 (RTN3) and obesity with hypertriglyceridemia in humans and animals, and Tg-RTN3 mice could be a suitable model for obesity and hypertriglyceridemia disease
- We identified elevated RTN3 will induce lipid droplets expansion;
- We found that RTN3-HSPA5 interaction activates SREBP1-c and induces obesity and TG accumulation.

#### What are the clinical implications?

- The present finding of a positive correlation between plasma RTN3 levels and TG accumulation may provide a novel biomarker for obesity and hypertriglyceridemia.
- Overexpression of RTN3 can induce the obesity and hypertriglyceridemia, which may bear clinical potential for treatment of obesity and hypertriglyceridemia.

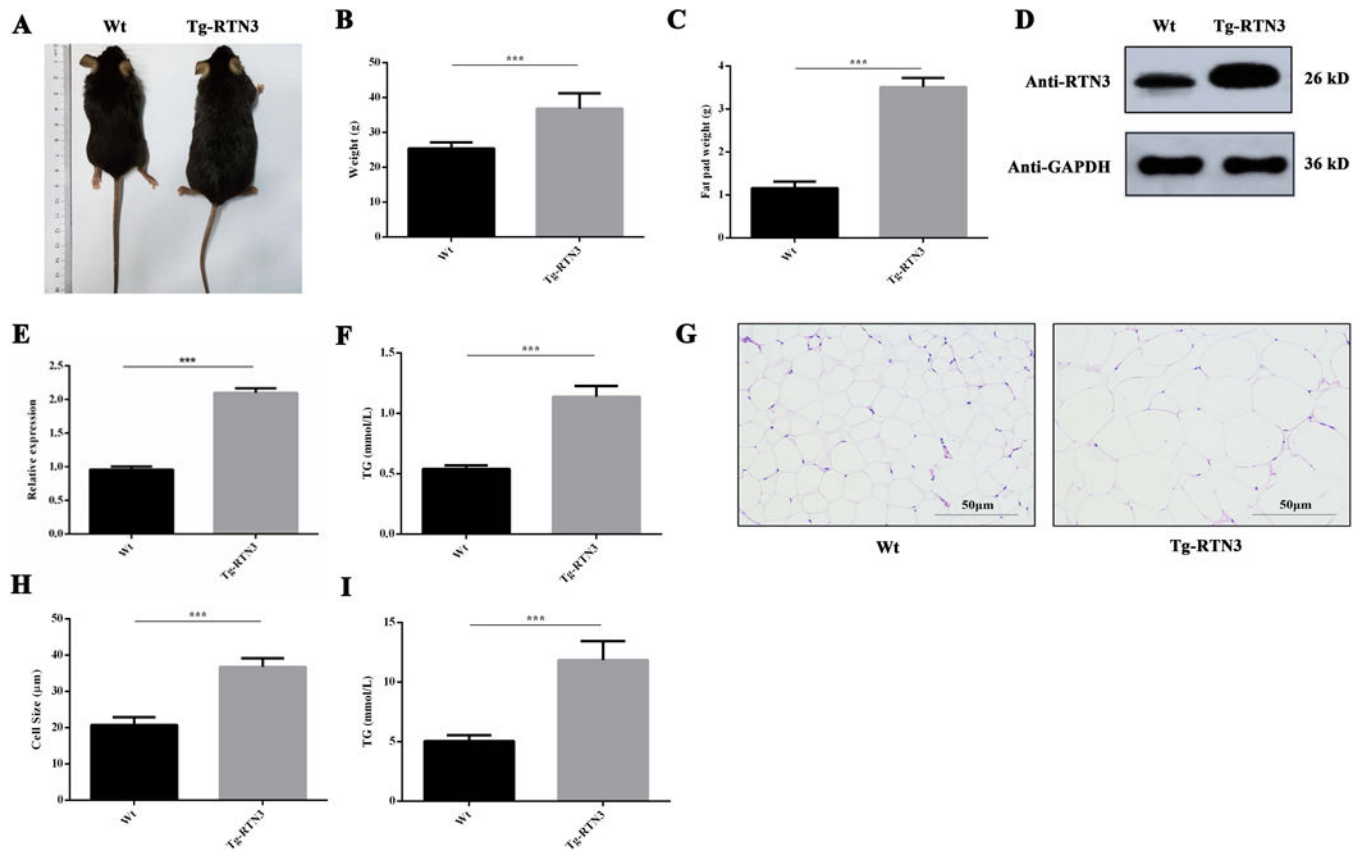


**Figure 1.**

Tg-RTN3 mice presented obesity and hypertriglyceridemia phenotypes. (A, B) The body shape and weight of Wt mice (n=7) and Tg mice (n=7). (C) The weight of epididymal fat tissue in Tg-RTN3 and Wt mice. (D, E) Western blot analysis showing RTN3 expression in Tg-RTN3 mice and Wt mice. (F) Peripheral blood TG levels of Tg-RTN3 mice (n=7) and Wt mice (n=7). (G, H) H&E staining analysis showing the size of fat cells in Tg-RTN3 mice and Wt mice. (I) Fat tissue TG levels in Tg-RTN3 mice (n=7) and Wt mice (n=7).

\*\*\*represents  $p < 0.001$ . All experiments were repeated at least three times. All the results represent the mean  $\pm$  SEM of at least 3 independent experiments in this study.

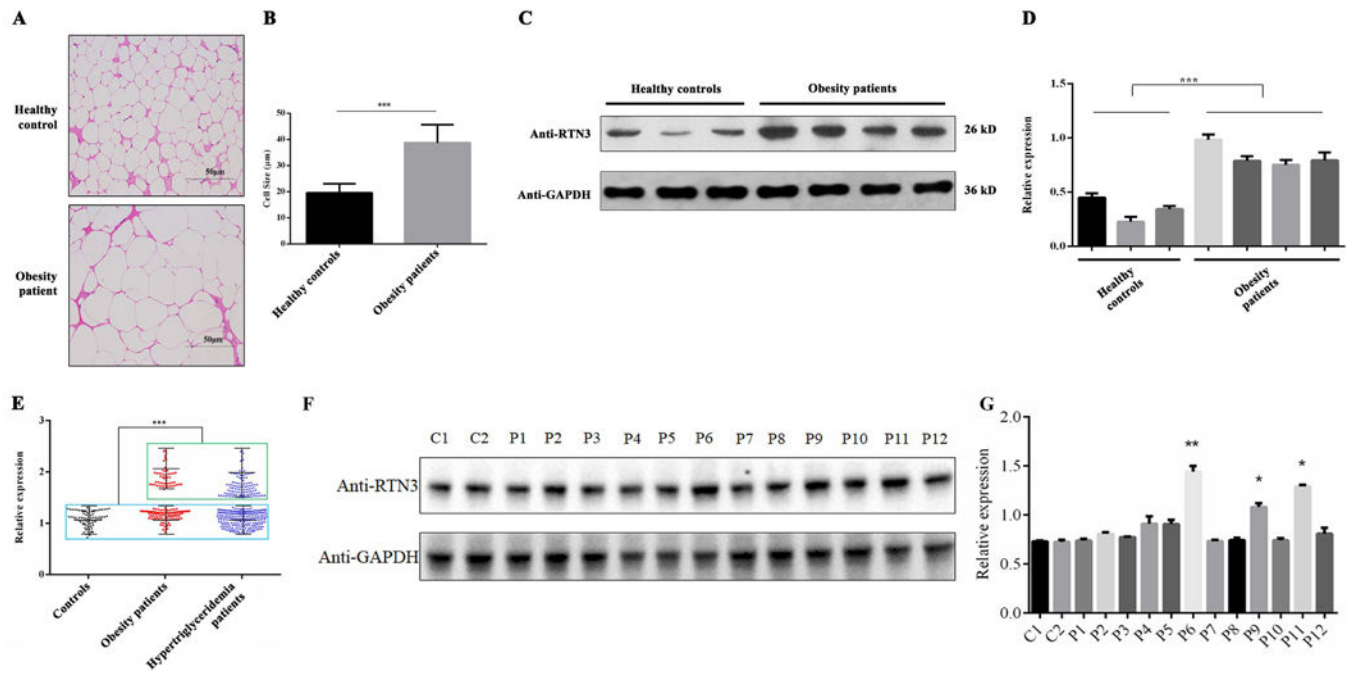


**Figure 2.**

RTN3 is highly expressed in obese and hypertriglyceridemia patients. (A, B) H&E staining analysis of fat cell size in normal individuals and obese patients. (C, D) Western blot analysis showing the levels of RTN3 in normal individuals (n=3) and obese patients (n=4). (E) Western blot analysis showing RTN3 levels in leukocytes from healthy controls (n=86), hypertriglyceridemia patients (n=343), and obese patients (n=149). Samples in Green Square showed higher expression of RTN3 and in Blue square showed normal expression of RTN3. (F, G) Western blot analysis showing RTN3 levels in fat tissue from normal individuals (C1 and C2) and hypertriglyceridemia patients (P1-P12). \* represents  $p < 0.05$ , \*\* represents  $p < 0.01$ , \*\*\* represents  $p < 0.001$ .

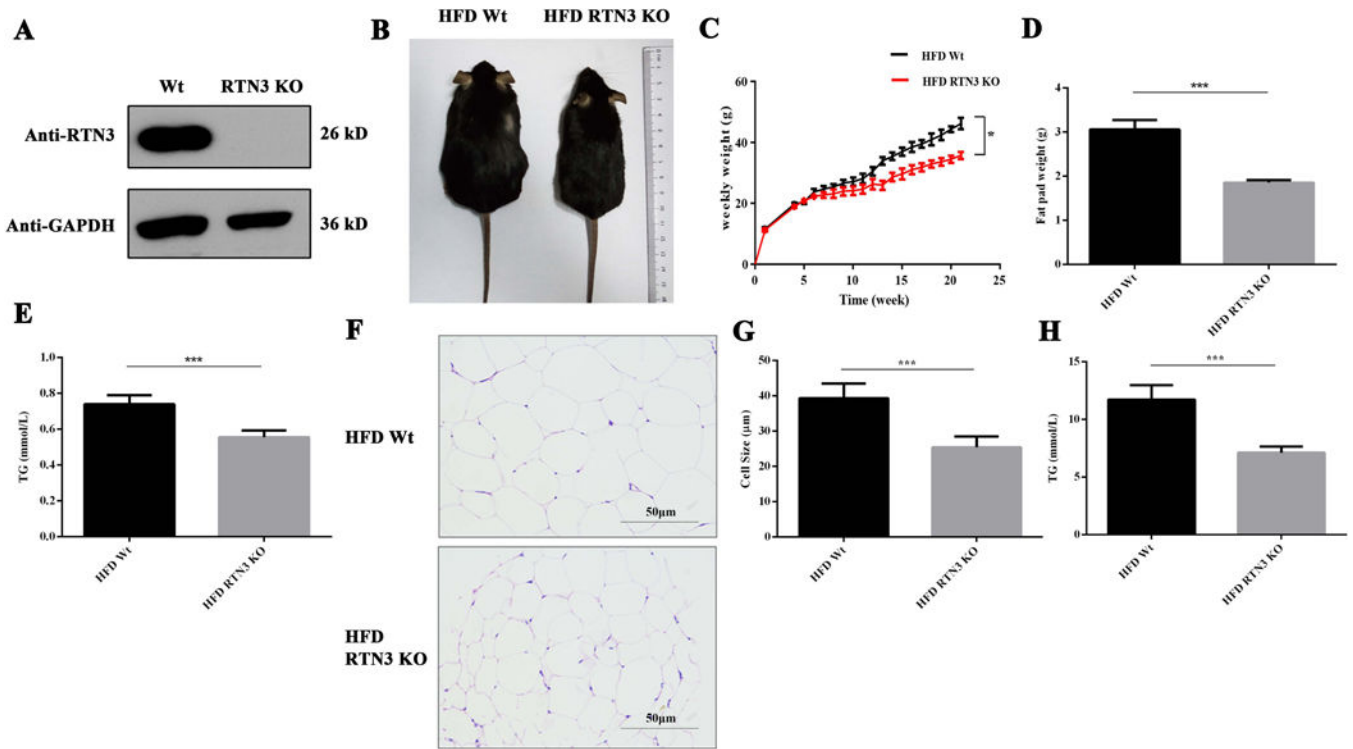


**Figure 3.** RTN3 deficiency leads to resistance against TG accumulation following a high-fat diet in mice. (A) Western blotting confirmed the RTN3-null mouse model. Data shows RTN3 homozygous knockout mice. (B) Example of differences in body size between WT and RTN3 KO mice after HFD feeding. (C) Body weight was measured weekly (WT n=9, KO n=9) and body weights were compared over time. (D) Weight analysis of epididymal fat tissue from RTN3 KO and Wt mice after HFD feeding. (E) Peripheral blood TG levels of RTN3 KO mice (n=7) and WT mice (n=7) after HFD feeding. (F, G) H&E staining analysis showing the size of fat cells in HFD normal mice and HFD RTN3 KO mice. (H) Fat tissue TG levels of HFD RTN3 KO mice (n=7) and HFD Wt mice (n=7). \* represents  $p < 0.05$ , \*\* represents  $p < 0.01$ , \*\*\* represents  $p < 0.001$ .



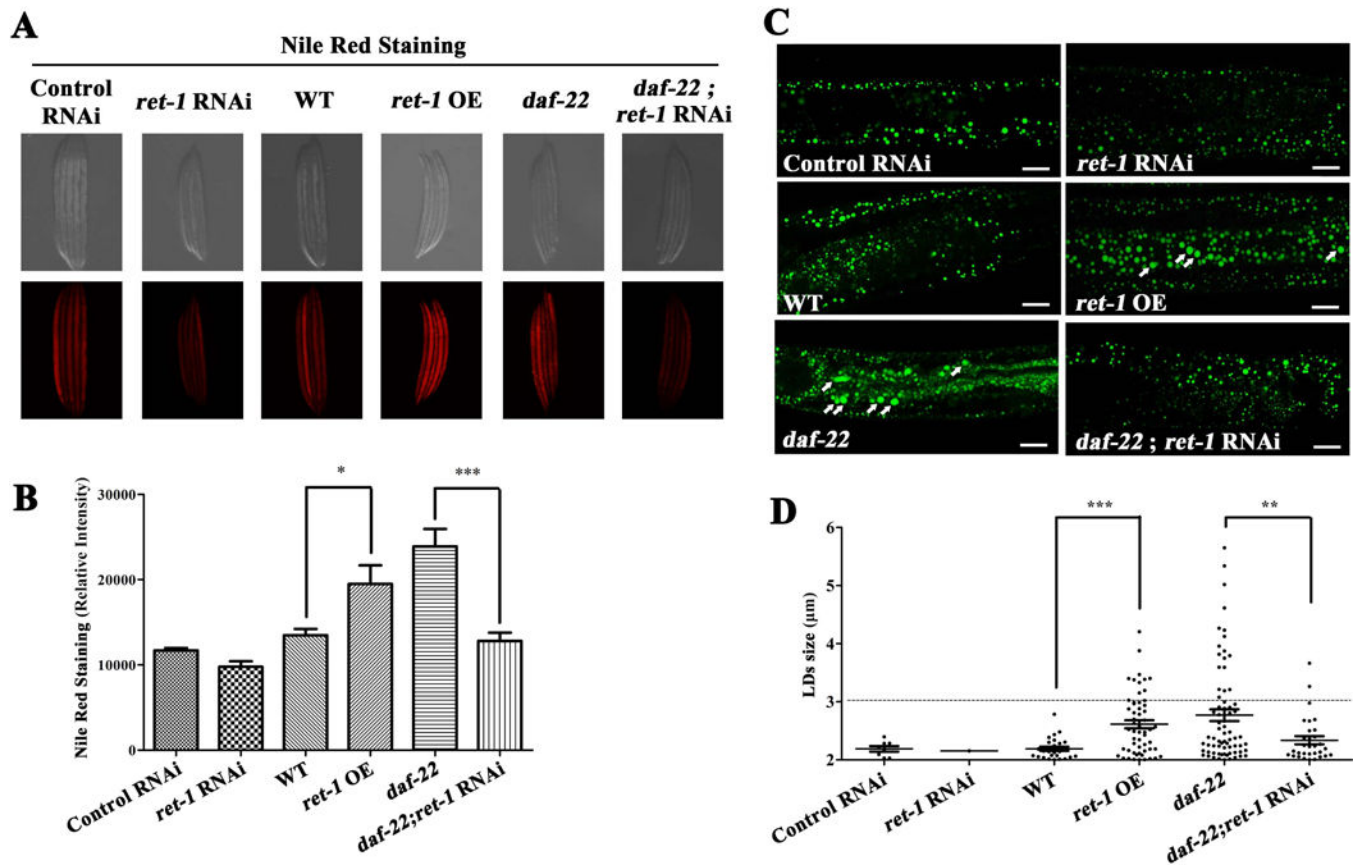


**Figure 4.**

RET-1 is required for LD expansion and TG accumulation in *C. elegans*. (A) Nile Red staining on fixed larval stage L4 nematodes. (B) Quantification of Nile Red staining (n=5). (C) BODIPY staining of nematodes. Bars: 10  $\mu$ m. (D) Quantification of BODIPY staining (n=5). \* represents  $p < 0.05$ , \*\* represents  $p < 0.01$ , \*\*\* represents  $p < 0.001$ ; ns represents not significant.

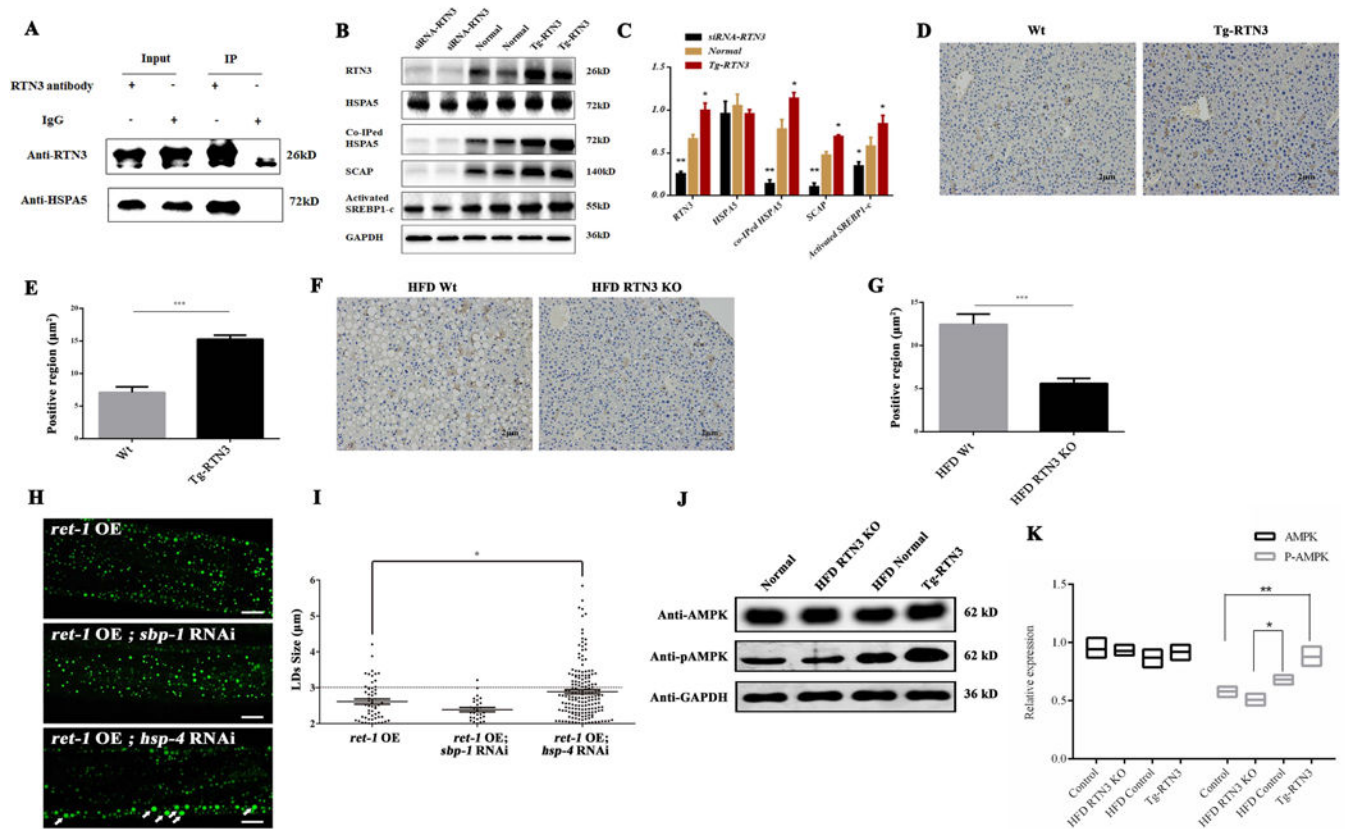


**Figure 5.** Increased RTN3 expression can competitively bind to HSPA5 and further activate SREBP-1c and AMPK. (A) Co-IP confirmed that RTN3 can interact with HSPA5 in mouse fat tissue. (B, C) Western blot and Co-IP analysis showing the levels of HSPA5, Co-IPed HSPA5, SCAP, and activated SREBP1c in 3T3L1 cells transfected with RTN3 plasmids and siRNA-RTN3 plasmids. (D, E, F, G) Immunohistochemistry analysis showing the levels of SREBP-1c in Tg-RTN3, Wt, HFD WT, and HFD RTN3 KO mice livers. (H,I) BODIPY staining of RNAi *hsp-4* and RNAi *sbp-1* in *ret-1* overexpression *C. elegans*. (J, K) Western blot analysis showing levels of AMPK and p-AMPK in HFD WT mice, HFD RTN3 KO mice, WT mice, and Tg-RTN3 mice. \* represents  $p < 0.05$ , \*\* represents  $p < 0.01$ , \*\*\* represents  $p < 0.001$ .

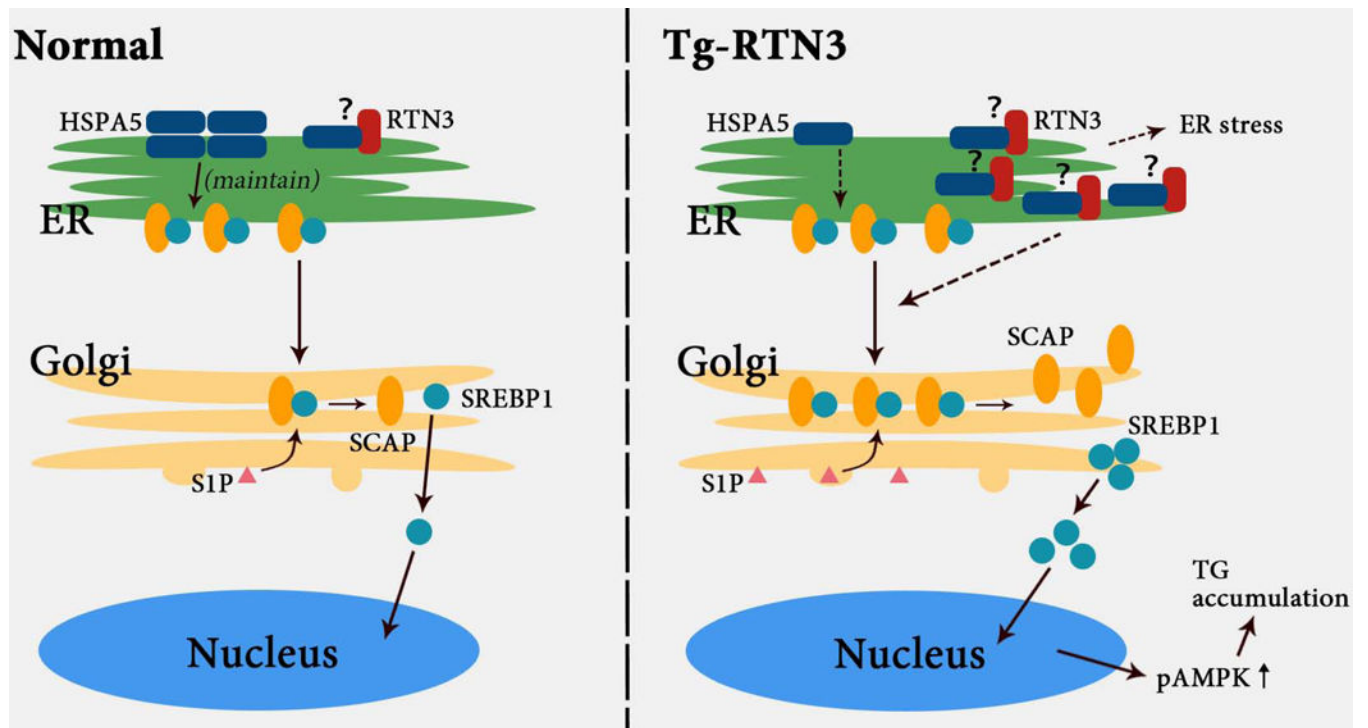


**Figure 6.** The potential mechanism of how higher RTN3 expression affects the accumulation of triglycerides in plasma and fat tissue.

**Table 1**

The clinic statistical data of patients

Characteristics	Healthy control (84)	Hypertriglyceridemia patient (343)	Obesity patients (149)
Age (years)	31.15 ±15.21	38.75±14.95	36.75±12.73
Gender(male/female)	49/35	160/183	61/88
TC (mmol/L)	6.15±3.96	5.89±2.32	6.23±2.94
TG (mmol/L)	1.05±0.80	11.26±7.90	7.82±5.17
HDL (mmol/L)	1.45±0.36	1.08±0.39	1.12±0.74
LDL (mmol/L)	3.32±1.83	3.13±2.19	3.03±2.05
CHD/AS	0	71	19

CHD: coronary heart disease; AS: atherosclerosis

Author Manuscript

Author Manuscript

Author Manuscript

Author Manuscript